Copyright © 2008 American Scientific Publishers
All rights reserved
Printed in the United States of America

Journal of Computational and Theoretical Nanoscience
Vol. 5, 1115–1119, 2008

Three-Dimensional Simulations of Quantum Confinement and Random Dopants Effects in Nanoscale nMOSFETs

G. Fiori*, S. Di Pascoli, and G. Iannaccone

Dipartimento di Ingegneria dell'Informazione, Università di Pisa, Via Caruso 16, I-56122, Pisa, Italy

The combined effect of quantum confinement at the Si/SiO_2 interface and the discrete distribution of dopants in the active area has been considered in ultrashort channel MOSFETs, via a numerical solution of the three-dimensional self-consistent Poisson/Schrödinger equation. Focusing our attention on the so-called "well tempered" bulk-Si n-MOSFETs with channel length of 25 and 50 nm proposed by D. Antoniadis, we have simulated a large number of devices with the same doping profile, but with different actual discrete distribution of impurities, and have extracted the threshold voltage distribution. We have found that the threshold voltage standard deviation is of the order of tens of millivolt, and that it is affected by quantum confinement in the channel.

Keywords: Poisson/Schrödinger, Random Dopant, Well-Tempered MOSFET, Threshold Voltage Distribution.

1. INTRODUCTION

Device simulation is a fundamental tool in CMOS technology development to understand and predict transistor behavior. To achieve this goal, modern simulators have to take into account effects that are relevant for present and future technology nodes, and that are going to have increasing relevance as geometries are reduced.

Indeed, in state of the art transistors, the number of ionized impurities is of the order of hundreds, and stochastic variations of the number and of the position of the dopants occur, due to the random nature of ion implantation and diffusion. These microscopic variations greatly affect macroscopic quantities such as off-state current and threshold voltage, as demonstrated experimentally in Ref. [1].

In order to understand, predict and control the effects of discrete dopants, analytical modeling and numerical simulations have been performed in the last decade. A simple one-dimensional analytical model that takes into account the fluctuations of the total number of dopants and of the positions, has been proposed in Refs. [2, 3], and considerably improved in Ref. [4]. Three-dimensional simulations, capable of taking into account the random position of ionized impurities in all directions, that is important in very short devices, have been performed in Refs. [5–7]. It is worth noticing that such works are based on semiclassical simulations, in which quantum effects are not considered at all.

However, devices with channel lengths of the order of tens of nanometers and oxide thickness in the range of 1–3 nm, are significantly affected by quantum confinement.[2,8] The high electric field in the direction perpendicular to the Si/SiO_2 interface, due to the reduced gate oxide thickness and the increased bulk doping, strongly confines electrons in the channel and induces well-separated 2D subbands. Such effect must be considered to make reliable prediction of device properties.

The influence of quantum effects on the dispersion of the threshold voltage has been addressed by Asenov[9] by means of the density gradient formalism.

Such approach, however, is a rude approximation of the self-consistent solution of the Poisson/Schrödinger equation, requires a previous calibration for the particular structure, and the error is not easily controllable in the case of rapidly varying potentials. Therefore, we propose to perform a full quantum simulation, based on the self-consistent solution of the Poisson/Schrödinger equation with density functional theory.

To this purpose we have developed a code for the simulation in three dimensions of MOSFETs with ultra-narrow channel, taking into account quantum confinement in the channel and depletion of the polysilicon gate. A controlled approximation allows to simplify the computation of the density of states in the channel.

We present results for the so-called "Well tempered" bulk-Si n-MOSFETs with channel length and width of 25 and 50 nm proposed by D. Antoniadis[10] as benchmark structures for the simulation of nanoscale MOSFETs. As we shall show, quantum confinement increases the

*Author to whom correspondence should be addressed.

RESEARCH ARTICLE

1546-1955/2008/5/1115/005
doi:10.1166/jctn.2008.009

threshold voltage by up to 290 mV for the 25 nm channel length device.

A description of the model and of the numerical methods is presented in Section 2. In Section 3 we present a discussion on the extraction of the threshold voltage and results on the threshold voltage shift due to quantum confinement. In the same section we discuss the effects of a discrete distribution of impurities on the threshold voltage, based on the simulation of a large number of devices with different atomistic doping profile. Conclusions are given in Section 4.

2. MODEL

The potential profile in the three-dimensional simulation domain shown in Figure 1 obeys the Poisson equation

$$\nabla[\epsilon(\vec{r})\nabla\phi(\vec{r})] = -q[p(\vec{r}) - n(\vec{r}) + N_D^+(\vec{r}) - N_A^-(\vec{r})] \quad (1)$$

where ϕ is the electrostatic potential, ϵ is the dielectric constant, p and n are the hole and electron densities, respectively, N_D^+ is the concentration of ionized donors and N_A^- is the concentration of ionized acceptors. Hole, acceptor and donor densities are computed in the whole domain with the semiclassical approximation, while the electron concentration in strongly confined regions is computed by solving the Schrödinger equation with density functional theory, with local density approximation.[11] In order to reduce computational requirements, the density of states is written as a sum of two dimensional subbands, obtained by solving the one-dimensional Schrödinger equation in the direction perpendicular to the Si/SiO_2 interface, for each grid point in the horizontal plane. The derivation of this approximation and an evaluation of the error can be found in Ref. [12]. The related error on the eigenvalues is always smaller 0.1%.

The Poisson/Schrödinger equation is solved self-consistently with the Newton-Raphson scheme with a predictor/corrector algorithm close to that proposed in Ref. [13]. In particular, to simplify the Jacobian and to achieve faster convergence, the Schrödinger equation is solved at the beginning of the Newton-Raphson cycle: the eigenfunctions are considered constant within the cycle, while eigenvalues are varied by a quantity equal to $q(\phi - \tilde{\phi})$, where $\tilde{\phi}$ is the potential used to solve the Schrödinger equation and ϕ is the potential at the current iteration. The electron density then becomes

$$n(x) = \frac{2k_B T m_t}{\pi\hbar^2} \times \sum_i |\psi_{li}|^2 \ln\left[1 + \exp\left(\frac{E_F - E_{li} + q(\tilde{\phi} - \phi)}{k_B T}\right)\right] + \frac{4k_B T\sqrt{m_l m_t}}{\pi\hbar^2} \times \sum_i |\psi_{ti}|^2 \ln\left[1 + \exp\left(\frac{E_F - E_{ti} + q(\tilde{\phi} - \phi)}{k_B T}\right)\right] \quad (2)$$

where anisotropy of the mass is considered and ψ_{li}, E_{li}, ψ_{ti} and E_{ti} are the eigenfunctions and eigenvalues obtained from the one-dimensional Schrödinger equation using the longitudinal effective mass m_l and the transverse effective mass m_t, respectively. The algorithm is then repeated cyclically until the two-norm of $\phi - \tilde{\phi}$ is smaller than a predetermined value.

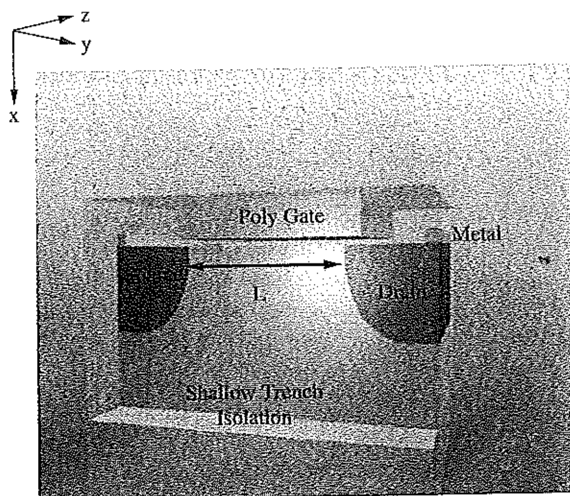

Fig. 1. Three-dimensional structure of the simulated MOSFETs.

3. RESULTS AND DISCUSSION

The structure considered in the simulations is depicted in Figure 1 and the doping profiles of the "Well tempered" MOSFETs suggested by D. Antoniadis[10] are shown in Figure 2 for the 25 and 50 nm channel length devices.

Source and drain doping profiles are gaussian, while a super halo doping is implanted in the channel in order to reduce charge sharing effects. In all the performed simulations gate tunneling current has not been considered, since we have verified that is negligeble as compared to the obtained drain-to-source current values.

3.1. Threshold Voltage Computation

In order to reduce the time required to perform a statistical simulation, we need to choose a convenient way to extract the threshold voltage V_T, without computing the complete I–V characteristic for each device.

One method to extract the threshold voltage is to compute the conductance g_0, which has the following approximate expression

$$g_0 \equiv \left.\frac{\partial I_D}{\partial V_{DS}}\right|_{V_{DS}=0} \approx \mu_n \frac{W}{L} C_{ox}(V_{GS} - V_T) \quad (3)$$

where μ_n is the electron mobility in the channel, C_{ox} is the oxide capacitance per unit area, W and L are the channel width and length, respectively, while V_{GS} and V_{DS} are the gate and the drain-to-source voltage.

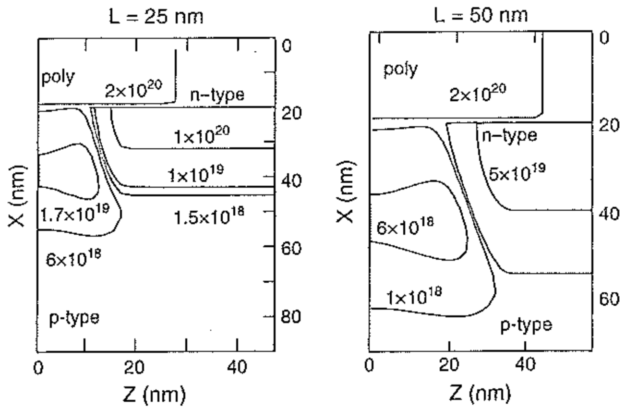

Fig. 2. Contour plot of the difference between donor and acceptor concentrations for MOSFETs with channel length of 25 and 50 nm. The profiles are symmetric so only the halves are shown. Units are cm^{-3}.

V_T can be then obtained as the intercept of the curve g_0–V_{GS} in the strong inversion region with the V_{GS} axis. The conductance is computed by solving a simplified continuity equation.[14] In particular the current density can be expressed as

$$\vec{J}_n = -qn\mu_n \nabla\phi_n \qquad (4)$$

where μ_n is the electron mobility and ϕ_n is the quasi fermi level for the electrons. If we now suppose to work at quasi equilibrium, (4) becomes,

$$\vec{J}_n = -qn_0\mu_n \nabla\phi_n \qquad (5)$$

where n_0 is the charge density computed for drain-to-source voltage equal to zero.

Considering a constant electron mobility and a null generation-recombination term, the continuity equation for the electrons reads,

$$\nabla \cdot J_n = 0 \qquad (6)$$

and substituting (5) in (6) we obtain

$$\nabla \cdot (n_0 \nabla\phi) = 0 \qquad (7)$$

The boundary condition for Eq. (7) are shown in Figure 3 for a region of the MOSFET containing the channel. A small voltage $\Delta\phi$ is applied between the source and the drain, while a zero current density is fixed through lateral faces of the region, imposing the gradient of the quasi Fermi level in the direction perpendicular to the surface equal to zero.

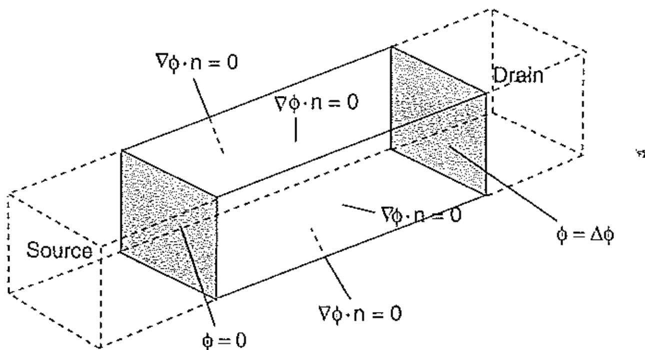

Fig. 3. Region considered for the calculation of conductance and associated boundary conditions.

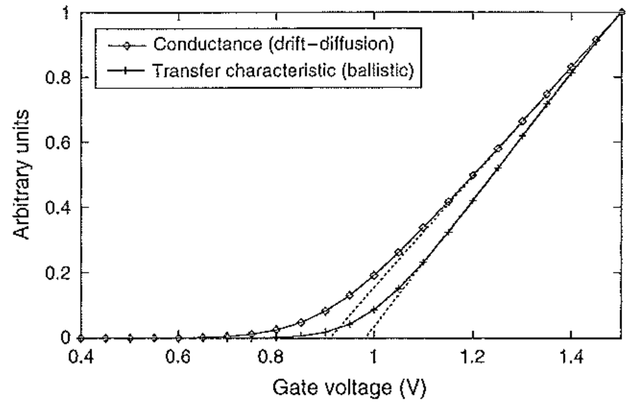

Fig. 4. Conductance versus V_{GS} for $V_{DS} = 0$ V and transfer characteristics for $V_{DS} = 10$ mV.

Another method is to derive the threshold voltage directly from the transfer characteristics, extracting the intersection of the line approximating the drain current as a function of the gate voltage at fixed V_{DS}. To this purpose, we have used a model widely explained in our previous work,[15] that describes the device behavior out of the equilibrium, considering fully ballistic transport in the channel

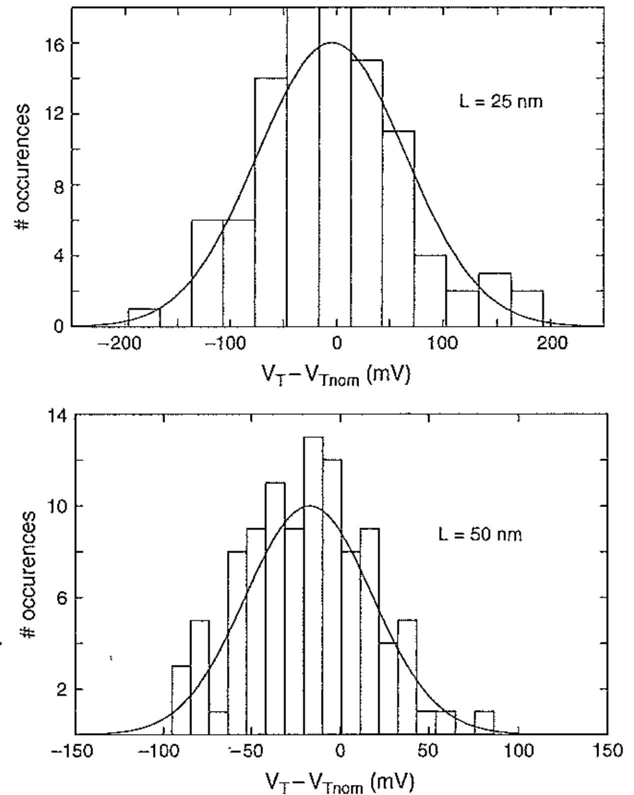

Fig. 5. Threshold voltage distribution in the two simulated devices: ($L = 25$ nm and $L = 50$ nm).

RESEARCH ARTICLE

Table I. V_{T_Q} and $V_{T_{sc}}$ are the quantum and semiclassical threshold voltage, σ_{sc} and σ_Q are the corresponding standard deviations, respectively. σ_s and σ_i are the standard deviations computed as in Ref. [4] using the 1D doping profile in the middle of the channel and the average 1D profile in the y–z plane.

Channel length L (nm)	$V_{T_Q} - V_{T_{sc}}$ (mV)	σ_s (mV)	σ_i (mV)	σ_{sc} (mV)	σ_Q (mV)	$\frac{\sigma_Q}{V_{T_{Qnom}}}$ (%)
25	287	32	33	58.57	69.8	7.56
50	219	14	14.9	32.43	35.9	6.81

(Fig. 4). Compared to the previous one, this approach is able to take into account drain-induced barrier lowering, but, on the other hand, has a much larger computational cost. We have indeed verified that the slope of g_0 as a function of V_{GS} does not depend on the particular impurity distribution, so that V_T can be obtained by computing g_0 for a single V_{GS}.[16]

This definition of V_T, however, can give a different value compared to other commonly used definitions.[2] Nevertheless, we believe that our evaluation of the V_T-shift due to quantum confinement is quantitatively accurate.

3.2. Threshold Voltage Dispersion

In nanoscale MOSFETs, the number of ionized impurities in the depletion region is of the order of hundreds. The threshold voltage is consequently very sensitive to intrinsic dopant fluctuations. For an accurate quantitative study of MOSFET behavior is therefore necessary to take into account this effect together with quantum confinement in the channel.

We have assumed that implanted ions in the channel obey the Poisson distribution. In particular, for each grid point we have considered the associated volume element and multiplied its volume ΔV by the nominal doping concentration. Then, a random number N' has been extracted with Poisson distribution and divided by ΔV in order to have the "actual" doping concentration in the volume element. The standard deviation of V_T has been then obtained by simulating a large number of devices with the same nominal doping, but with different actual dopant distribution. Figure 5 shows the distribution of threshold voltage computed on an ensemble of 100 nominally identical devices, where $V_{T_{Qnom}}$ is the quantum computed threshold voltage in case of nominal doping, while in Table I the standard deviations of the threshold voltage σ_{VT} are shown.

The considered number of simulated devices is a good compromise between precision and computational burden. Indeed the standard deviation of the error on σ_{VT} is about 7%, which is still accurate.

In Table I, the first column represents the threshold voltage shift in case of nominal doping due to quantum effects: $V_{T_{sc}}$ and V_{T_Q} are the threshold voltage computed with semiclassical and quantum models, respectively. σ_{sc} and σ_Q are the corresponding standard deviations respectively, while σ_s and σ_i are the standard deviation computed with the analytical model described in Ref. [3] using respectively the one-dimensional doping profile extracted in the middle of the channel and the one-dimensional profile derived from the average integration of the three-dimensional profile over the y–z plane.

As it can be noted, the standard deviation computed by means of quantum model is larger than the one computed semiclassically since the threshold voltage standard deviation is a rising monotonic function of the oxide thickness, and quantum confinement effects produce an increase of the effective oxide thickness itself. Moreover, analytical models[2] largely underestimate the standard deviation, since do not consider the charge sharing effect that are relevant at these geometries.

For the two structures, we have also computed the threshold voltage standard deviation as a function of the

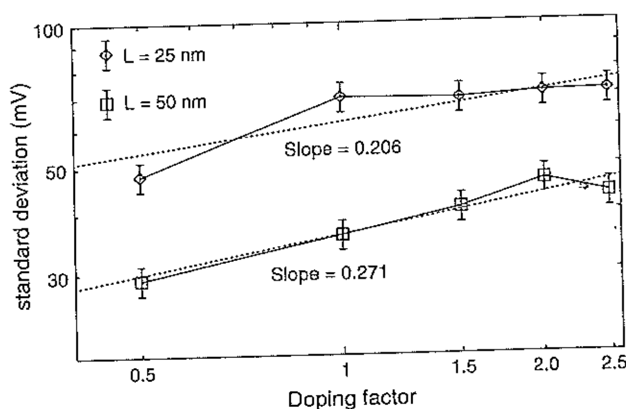

Fig. 6. Threshold voltage standard deviation as a function of the multiplying factor of the doping profile.

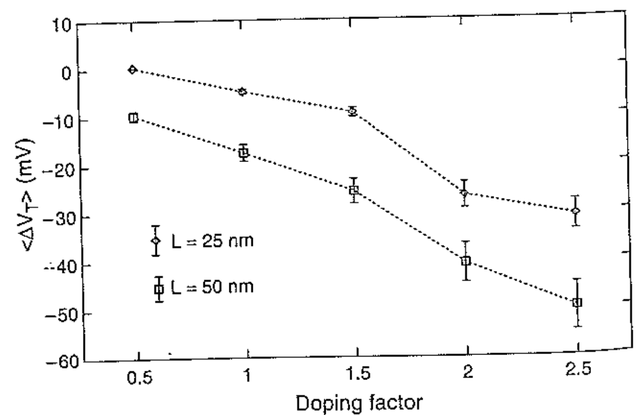

Fig. 7. Mean value of the threshold voltage variation (ΔV_T) as a function of the multiplying factor of the doping profile.

RESEARCH ARTICLE

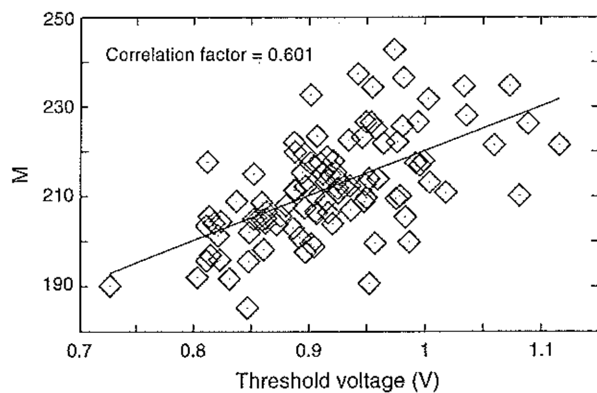

Fig. 8. Scatter plot of M versus V_T for the $L = 25$ nm device for 100 devices, and least mean square fitting line. The correlation coefficient is 0.601.

doping concentration (Fig. 6). In particular we have multiplied the doping profile for a factor and then we have computed the standard deviation as explained above.

The slopes of the least mean square fitting lines differ from that computed using the mono-dimensional analytical model and equal to 0.25 as described in Refs. [2, 3 and 4]. Extracting the 1D doping profile in the middle of the channel, the analytical simulations have yielded slopes equal to 0.262 and 0.247 for the devices with channel length equal to 25 and 50 nm respectively. Indeed in our three-dimensional simulator, charge sharing effects are taken into account as well as quantum confinement.

In Figure 7 is shown the mean value of the threshold voltage variation ($\Delta V_T = V_{T_Q} - V_{T_{Qnom}}$) as a function of the doping factor: as expected theoretically[2] it decreases for increasing doping factor. Just to investigate the influence of dopant position on the threshold voltage, we have computed for each randomly generated dopant profile and for the 25 nm case, the term M, defined as

$$M = \int_0^{W_d} dx \int_0^W dy \int_{-\frac{L}{2}}^{\frac{L}{2}} dz \left(1 - \frac{x}{W_d}\right) N_A(x, y, z) \qquad (8)$$

where W_d is the depletion region length.

In Figure 8 the scatter plot of M versus V_{T_Q} for each sample is shown. As can be seen, the correlation is about 0.601, that is quite far from 0.964 found in Ref. [17] in case of constant bulk doping.

Indeed (8) not only confers a larger weight to shallower impurities, but also tacitly assumes that only the position of impurities along x affects threshold voltage dispersion. The scatter plot suggests that in the case of three-dimensional doping profile also the position of impurities on the y–z plane is relevant: this will require further investigation.

4. CONCLUSION

We have developed a three-dimensional Poisson/Schrödinger solver and we have performed a statistical simulation of two nanoscale "Well tempered" MOSFETs.

Our code has allowed us to take into account simultaneously the effects on threshold voltage of the random distribution of dopants and of quantum confinement in the channel.

We have shown that an accurate evolution of the dispersion of threshold voltage requires quantum confinement to be properly taken into account.

Geometrical dispersion can be another source of threshold voltage fluctuations. The dispersion of V_T for devices with channel length below 30 nm due to oxide fluctuations is comparable to that due to random discrete dopants, as shown in Ref. [18]. However geometrical and random dopants fluctuations are independent, so a separate study is justified.

Acknowledgments: Support from the European Commission throughout the PullNANO Project (Contract no. 026828) is gratefully acknowledged.

References

1. T. Mizuno, J. Okamura, and A. Toriumi, *IEEE Trans. Electron Devices* 41, 2116 (1994).
2. Y. Taur and T. H. Ning (eds.), Fundamentals of Modern VLSI Devices, Cambridge University Press, Cambridge, UK (1998), pp. 194–202.
3. K. Takeuchi, T. Tatsumi, and A. Furukawa, *IEDM Tech. Digest* 1, 841 (1997).
4. P. A. Stolk, F. P. Widdershovwn, and D. B. M. Klaassen, *IEEE Trans. Electron Devices* 45, 1960 (1998).
5. H.-S. Wong and Y. Taur, *IEDM Tech. Digest* 1, 705 (1993).
6. A. Asenov, *IEEE Trans. Electron Devices* 45, 2505 (1998).
7. D. J. Frank, Y. Taur, M. Ieong, and H.-S. P. Wong, *VLSI Technology Dig. Tech. Papers* 1, 169 (1999).
8. Y. Taur, D. A. Buchanan, W. Chen, D. J. Frank, K. E. Ismail, S. H. Lo, G. A. Sail-Lalasz, R. G. Viswanathan, H. J. C. Wann, S. J. Wind, and H. S. Wong, *Proc. IEEE* 85, 486 (1997).
9. A. Asenov, G. Slavcheva, A. R. Brown, J. H. Davies, and S. Saini, *IEEE Trans. Electron Devices* 48, 722 (2001).
10. http://www-mtl.mit.edu/Well.
11. J. C. Inkson (ed.), Many-Body Theory of Solids, Plenum, New York (1984), pp. 265–286.
12. G. Fiori and G. Iannaccone, *Nanotechnology* 13, 294 (2002).
13. A. Trellakis, A. T. Galick, A. Pacelli, and U. Ravaioli, *J. Appl. Phys.* 81, 7800 (1997).
14. A. Asenov, *Proceedings of IWCE* (1998), pp. 263–266.
15. G. Fiori and G. Iannaccone, *Appl. Phys. Letters* 81, 3672 (2002).
16. E. Amirante and G. Iannaccone, *IEEE-NANO 2002 Tech. Dig.* (2002), p. 197.
17. G. Fiori and G. Iannaccone, *Journal of Computational Electronics* 2, 123 (2003).
18. A. Asenov, S. Kaya, and J. H. Davies, *IEEE Trans. Electron Devices* 49, 112 (2002).

Received: 28 February 2007. Accepted: 3 May 2007.

RESEARCH ARTICLE